# Chapter 5

# Growth of AAO Assisted CNT Arrays

## 5.1 Introduction

In the past decade, carbon nanotubes (CNTs) have become one of the most promising candidates for field electron emitters to be used in future generations of cold-cathode flat panel displays and various vacuum microelectronic devices because of their excellent field emission properties[Iijima 1991-56; Saito 2000-169; Jonge 2002-393]. They exhibit several favorable characteristics as an electron-emitting material, such as a high aspect ratio, small radius of curvature, high chemical inertness, high thermal stability, and high mechanical strength. For the practical application to field emission displays (FEDs) the growth of vertically aligned CNT arrays on a large area with high packing density and ordered arrangement is necessary. As for this requirement template methods are widely applied to produce well aligned and mono-dispersed CNT arrays. Ordered arrays of CNTs have been fabricated by using nanoporous anodic aluminum oxide (AAO) membranes as the template by several research groups[Kyotani 1996-2109; Li 1999-367; Iwasaki 1999-2044; Suh 1999-2047; Yao 2001-11395; Bae 2002-277]. Nanoporous AAO, which consists of vertical pore channel arrays with a hexagonal packing structure, was obtained by anodic oxidation of aluminum in an acidic electrolyte[Jessensky 1998-1178]. The diameter of the self-ordered nanopores is tunable in the range of ten to several hundred nanometers, because the pore diameter is dependent upon anodization parameters, such as polarization voltage, bath temperature, electrolyte species, and electrolyte concentration[Li 1998-6023], making AAO an ideal template for fabricating ordered arrays of nanostructured materials.

In the fabrication of CNTs assisted by nanoporous AAO templates, the obtained nanotubes generally have a very uniform diameter, vertical alignment, ordered arrangement, and very high packing density, which are the duplicate of the AAO pore channels. Selective growth of CNTs within the AAO nanopores usually requires pre-deposition processes of metal catalysts in the pore bottom and a high-temperature thermal chemical vapor deposition (CVD) process for catalyst pyrolysis of hydrocarbon precursors to grow CNTs. CVD enhanced by plasma is another potential alternative to dissociate the precursor gases with more efficiency. In this study, we propose the preparation of CNT arrays in AAO templates by the microwave plasma electron cyclotron resonance CVD (ECR-CVD). It is well known that the microwave plasma ECR-CVD with a high plasma density has the advantages of a high dissociation percentage of the precursor gas and a high uniformity of the plasma energy distribution[Lin 2002-922; Sung 1999-197], and was generally used for large area dry etching, surface cleaning, or thin film deposition. By using the microwave plasma ECR-CVD instead of the thermal decomposition, well-aligned CNT arrays have been successfully synthesized using the nanoporous AAO membrane as a template.

## 5.2 Integration of AAO and CNTs

For the preparation of the AAO template, an aluminum film of about 6 μm in thickness was first deposited on the *p*-silicon (100) wafer by thermal evaporation. The two-step anodization[Masuda 1995-1466; 1996-L126], which has been depicted in detail in Chapter 4, was used to prepare ordered pore channel arrays of AAO. Anodization was first carried out in a 0.3 M oxalic acid ($H_2C_2O_4$) solution at 21 °C under a constant polarization voltage of 40 V for 30 min. The resulting nanoporous AAO about 4.3 μm in thickness was then removed by wet chemical etching at 60 °C with a mixed solution of phosphoric acid ($H_3PO_4$) and chromic acid ($CrO_3$), and thereby a relatively ordered indent pattern was produced on the surface of the aluminum film. The second anodization of the pre-patterned aluminum film was then performed for 5 min under the same anodization condition as the first one. At the end of the second anodization, the voltage was dropped gradually from 40 to 10 V by 1 V steps. The decrease of polarization voltage accompanied the decrease of the alumina barrier thickness under each pore bottom. After the voltage drop process, the pore diameter of the AAO template was widened in a 5 vol.% phosphoric acid solution for 60 min. Figure 5-1(a) shows the top-view field-emission scanning electron microscopy (FE-SEM) (Hitachi S-4000) image of the nanoporous AAO film after the two-step anodization and pore widening. The self-organized nanopores with a uniform size distribution have a pore diameter about 60 nm and an interpore distance about 100 nm. The AAO nanopores do not show a long-range ordering, but within a pore array domain, ordered nanopore with a hexagonal arrangement is clearly observed. Figure 5-1(b) is the cross-sectional view

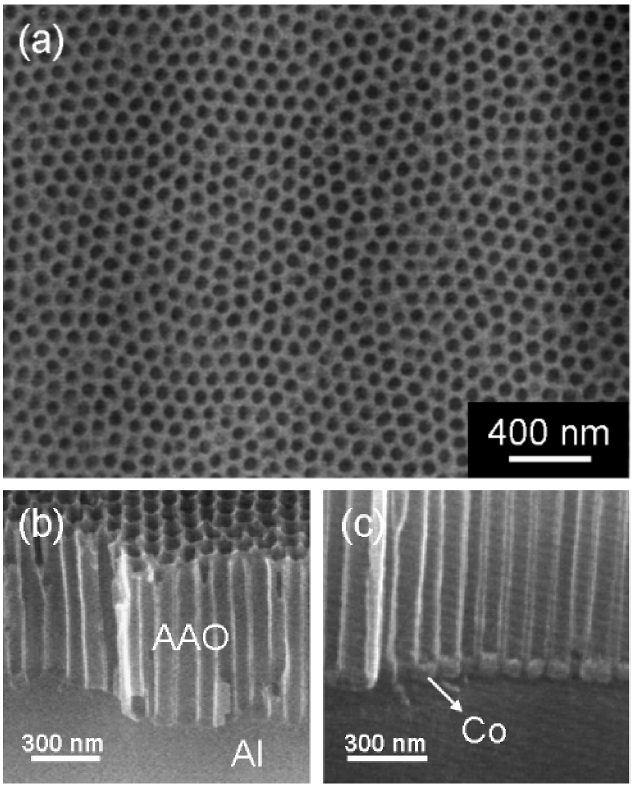

**Figure 5-1** (a) Top-view FE-SEM image of the nanoporous AAO film after pore widening in a 5 vol.% phosphoric acid solution for 60 min. Cross-sectional view FE-SEM images of the AAO film (b) before and (c) after cobalt electroplating.

of the AAO film. The depth of the straight cylindrical pores is about 740 nm. Moreover, it is obvious that the insulative alumina barrier layer under each pore bottom was removed completely during the pore widening step.

Before CNT growth, the cobalt catalyst was electrochemically deposited at the pore bottom in an electrolyte of 5 wt.% cobaltous sulfate ($CoSO_4{\cdot}7H_2O$) and 2 wt.% boric acid ($H_3BO_3$) by applying 12.3 $V_{rms}$ ac voltage for 1 min. After the cobalt electroplating uniform catalyst particles were deposited at the AAO pore bottom [see Figure 5-1(c)]. Finally, the catalyst pretreatment and the CNT growth were all carried out in a microwave plasma (2.45 GHz) ECR-CVD system under 875-Gauss magnetic field strength. Figure 3-3 shows a schematic diagram of the microwave plasma ECR-CVD system. The deposition conditions for the CNT growth were: microwave power 700 W, -150 V substrate bias, working pressure $2\times10^{-3}$ Torr, deposition temperature 600 $^{o}$C, $CH_4$:$H_2$ ratio = 11:11 sccm, and deposition time 7-30 min. The detailed conditions for the synthesis of CNTs are summarized in Table 5-1.

Lee *et al.*[Lee 2001-479] have reported the growth of CNTs in the AAO template with or without deposition of cobalt in the pore bottom as the catalyst. It was suggested that

**Table 5-1** Experimental conditions for the CNT growth on AAO template.

| **Sample** | **A** | **B** | **C** |
|---|---|---|---|
| **Microwave power** | 700 W | 700 W | 700 W |
| **Substrate bias** | -150 V | -150 V | -150 V |
| **Working pressure** | 2 mTorr | 2 mTorr | 2 mTorr |
| **Deposition temperature** | 600 °C | 600 °C | 600 °C |
| **$CH_4$ flow rate** | 11 sccm | 11 sccm | 11 sccm |
| **$H_2$ flow rate** | 11 sccm | 11 sccm | 11 sccm |
| **Growth time** | 7 min | 15 min | 30 min |

AAO as well as cobalt catalyst all play an important role on the pyrolysis of hydrocarbon precursors. CNTs were only grown in the pore channels of the AAO template when cobalt was not present, but these tubes have a very poor crystallinity [Kyotani 1996-2109; Bae 2002-277; Sui 2001-1523]. When the cobalt catalyst was deposited into the pores, both AAO and cobalt played important role to assist the growth of the CNTs. Because cobalt is a much more active catalyst for hydrocarbon decomposition[Jeong 2001-2052], the catalyst role of cobalt was dominant. The well-graphitized CNTs grew out of the pores due to a high growth rate and entwined above the pores. Figure 5-2 shows the side-view FE-SEM images of the cobalt-catalyzed CNTs grown on the AAO template by using the microwave plasma ECR-CVD. Similar to previous works, the CNTs also grew out of the pores, as shown in Figure 5-2, but the tubes aligned vertically to the AAO surface with little entanglement. In the earlier stage of the growth, the template effect of the AAO nanopores constrains the tubes to grow along the axis of the pores, resulting in the growth of the well-aligned tubes. After extending out of the pores, the overgrown CNTs remained the vertical growth direction due to the applied dc bias and the plasma induced electric field (self-bias) in the ECR plasma environment. The electrostatic force would force the exposed CNTs to align with the electric field[Bower 2000-830]. By using the AAO template, the CNTs of a very high packing density ($5\text{-}8\times10^9$ tubes/$cm^2$) are highly uniform in diameter with an average of about 75 nm, which is coincided with the pore size of the AAO template. However, the diameter of tubes is lager than that of the AAO pores before the CNT growth shown in Figure 5-1. This is possibly due to water loss in the AAO template from heating during the CVD process resulting in the enlargement of AAO pores[Suh 1999-2047].

From Figure 5-2, it can be clearly seen that the length of the CNTs increases with

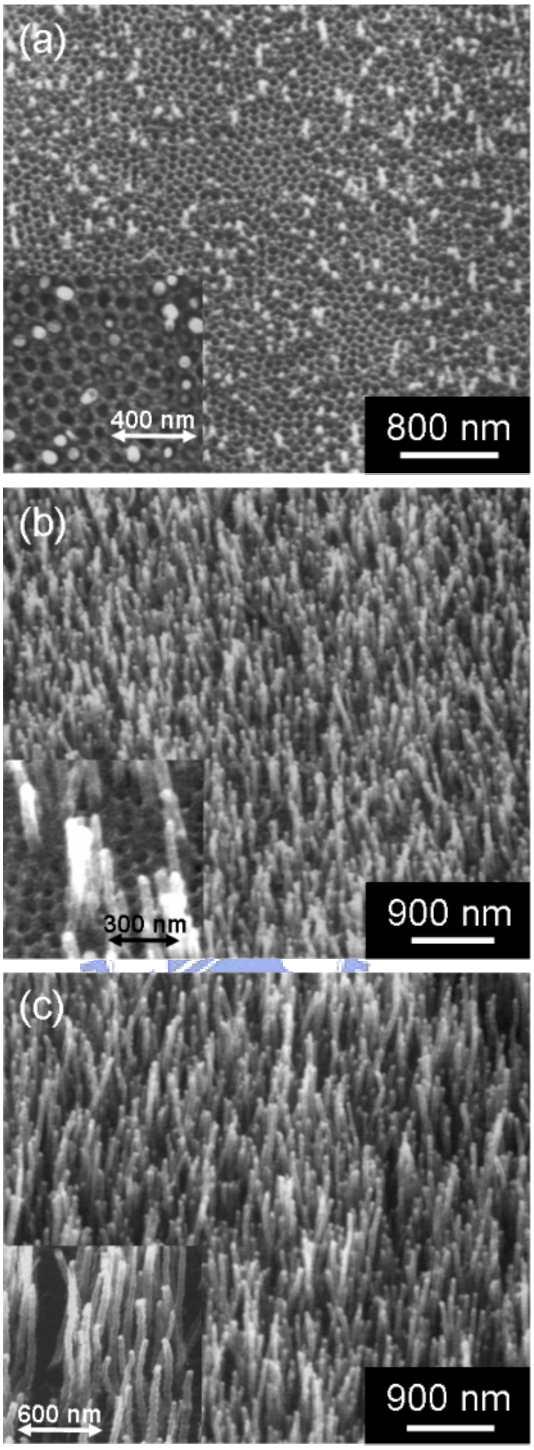

**Figure 5-2** Side-view FE-SEM images of the cobalt-catalyzed CNTs grown on the AAO template by using the ECR-CVD for (a) 7 min (sample A), (b) 15 min (sample B), and (c) 30 min (sample C). The insets show the close-up view of the CNTs grown out of the AAO template pores.

the growth time. As seen in Figure 5-2(a), most of the CNTs are shorter than the depth of pore channels after CNT growth of 7 min, and only a few tubes are observed to extend over the pores. After 15 min growth [see Figure 5-2(b)], it is obvious that the almost all the CNTs grew out of the pores, and the overgrowth length was about

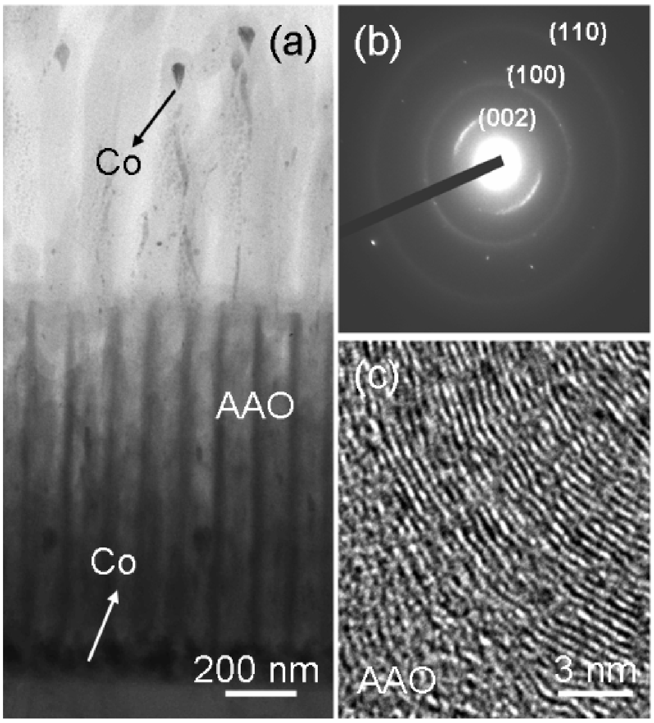

**Figure 5-3** (a) Cross-sectional TEM image of the very sample shown in Figure 5-2(b). The surface was covered with an amorphous silicon film to protect the exposed CNTs. (b) Electron diffraction pattern recorded from the overgrown part of the tubes shown in (a). (c) Plan-view HRTEM image of the walls of a graphitized CNT inlaid in an AAO pore.

300-700 nm. In the case of growth of 30 min [see Figure 5-2(c)], most of the tubes above the template had a length of 700 nm-1.5 μm. If the growth time was increased further, the tube length would not increase any longer, suggesting the cobalt catalyst was possibly poisoned[Qian 2003-878]. In the fabrication of triode field emitters using CNTs, one of the challenges is to control the length of aligned CNTs in the submicron scale without the overgrowth from the gate hole[Lee 2001-479]. The growth rate of CNTs in the AAO template by ECR-CVD is considerably low (< 100 nm/min), and, therefore, the tube length can be reliably controlled via the growth time. Thus the CNTs are potentially suitable for the field emitter applications.

The growth mechanism of CNTs prepared by the catalytic decomposition of hydrocarbon vapors has been divided into either tip- or base-growth[Baker 1989-315]. Figure 5-3(a) shows a cross-sectional transmission electron microscopy (TEM) (JEOL JEM-2010F) image of the sample shown in Figure 5-2(b). It is obvious that the cobalt catalyst particles are encapsulated at the tips of tubes and covered by graphitic caps. Although residual cobalt catalyst can also be observed in the tube base, the growth mechanism of the CNTs tends to be the tip-growth rather than base-growth for the present case. With regard to the base-growth, the precursor gases must continuously transport to the cobalt catalyst at pore bottom. If the gas diffusion is blocked, the catalytic growth of CNTs will be terminated. However, under the experimental condition, the nanopores are compactly filled with multi-walled CNTs and, moreover, the tubes have a closed end. The encapsulated cobalt nanoparticles at their tips can block the mass transfer of precursor gases implying that the base-growth is unfavorable. In the tip-growth, the gas diffusion will not be obstructed because the CNT growing site is at the tip of the tubes.

Figure 5-3(b) shows a selected-area electron diffraction pattern recorded from the overgrown part of the tubes shown in Figure 5-3(a). Three diffraction rings can be clearly identified to be (002), (100), and (110) of graphite. The diffraction pattern suggests that the tubes have a graphitic form with an inter-wall distance ($d_{002}$) of approximately 3.6 Å, which is larger than the inter-planar separation of graphite ($d_{002}$ = 3.35 Å). The larger inter-wall distance results from the curvature of the graphitic walls. Figure 5-3(c) is a plan-view high-resolution TEM (HRTEM) image showing a CNT inlaid in a pore of the AAO template. Since the tube has a relatively large diameter, only a part of the tube is shown in this figure. The tube is composed of about 70-80 graphitic walls, and the tube size is strongly defined by the AAO pore geometry. It should be noted that the number of the graphitic layers is independent on the growth time, and this is unlike the layer-by-layer growth mechanism proposed by Yao *et al.*[Yao 2001-11395]. They found that when the AAO was used alone to act as a catalyst to grow CNTs, the thickness of tube walls increased with increasing the growth time, inferring that the graphite was deposited layer-by-layer on the inner wall of the AAO pore. In regard to the cobalt-catalyzed growth of CNTs, increase of the growth time always leads to the increase the tube length as shown in Figure 5-2. Therefore, we believe that the catalyst role of AAO is minor in the presence of cobalt catalyst under our experimental conditions.

## 5.3 Field emission properties

Figure 3-4 shows the instrument setup and the test configuration used during field emission characterization. Measurements were conducted by the simple diode configuration and performed in a vacuum about $10^{-6}$ Torr. The distance between the CNTs and the anode was about 100 μm. The field emission current density ($J$) as a function of electric field ($E$) for the AAO template based CNTs of three different lengths

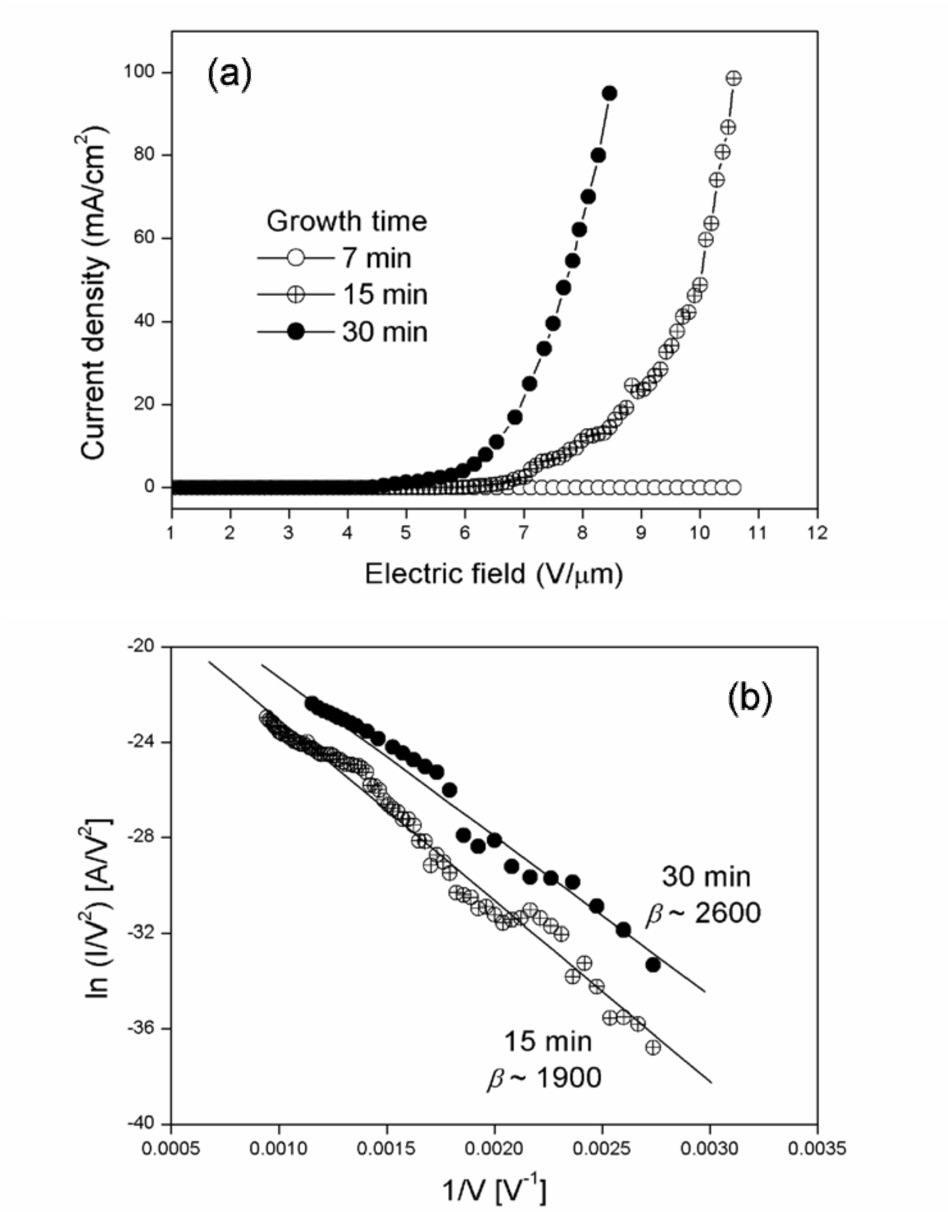

**Figure 5-4** (a) Field emission current density as a function of electric field for the CNTs grown in the AAO nanopores. (b) Corresponding Fowler-Nordheim plots of the data shown in (a).

is shown in Figure 5-4(a). It is obvious that the CNTs grown for 30 min (overgrown length: 700 nm-1.5 μm) show better field emission properties than that grown for 15 min (overgrown length: 300-700 nm) and 7 min. The current density of the CNTs grown for 7 min is too low (< 3 μA/cm$^2$) to be observed. The *J-E* data were analyzed by applying the Fowler-Nordheim (F-N) equation:

$$J = \frac{A\beta^2 V^2}{d^2 \varphi} \exp(-\frac{B d \varphi^{3/2}}{\beta V}) \qquad (5.1)$$

where $A = 1.54\times10^{-10}$ (A V$^{-2}$ eV), $B = 6.83\times10^{9}$ (V eV$^{-3/2}$ m$^{-1}$), $V$ is the applied voltage, $\beta$ is the field enhancement factor, $d$ is the distance between cathode and anode, and $\varphi$ is the work function of CNT. For the emitters following the F-N theory, the plot of $\ln(I/V^2)$ versus $1/V$ gives a straight line. As shown in Figure 5-4(b), the F-N plots corresponding to the $J$-$E$ curves show approximate linear relationship, revealing that the emission current is really caused by the quantum tunneling effect. From these plots, the $\beta$ values were computed by following equation:

$$\beta = -\frac{Bd\varphi^{3/2}}{S} \tag{5.2}$$

where $S$ is the slope of the FN plot. By assuming a CNT work function of 5 eV, the $\beta$ values calculated for the CNTs grown for 30 min and 15 min are approximately 2600 and 1900, respectively. The $\beta$ values are similar to the values for CNTs grown on an AAO template by Suh *et al.*[Suh 2002-2392]. It was concluded that the field emission is optimal ($\beta$ ~ 2650) when the exposed tube length is similar to the intertube distance, which was about 100 nm in their work. In our experiments, the tube packing density is obviously lower (CNT filled ratio of pores about 70%) and results in higher intertube distances. Therefore, the optimal field emission was obtained at an overgrown length above 1 μm. In order to avoid the field-screening effect[Nilsson 2000-2071], a lower packing density of CNTs is favorable.

## 5.4 Summary

The vertically aligned and well-graphitized CNT arrays can be successfully synthesized in the nanopores of the AAO template by using the microwave plasma ECR-CVD. Both the AAO template effect and the dc bias as well as the plasma induced self-bias contribute to the vertical alignment of the tubes. The obtained CNT arrays have a very high packing density (as high as $10^9$ tubes/cm$^2$) and a narrow diameter distribution (about 75 nm), which are in accordance with the pore arrays of AAO template. The tube growth was catalyzed by the pre-deposited cobalt catalyst inside the nanopores rather than the AAO template, and the tubes encapsulate cobalt particles at their tips suggesting the tip growth mechanism. These CNTs are multi-walled and well-graphitized and have good field emission properties.